Tunable absorption of $Au-Al_2O_3$ nanocermet thin films and its morphology

S. Hazra[a)]
Surface Physics Division, Saha Institute of Nuclear Physics, 1/AF Bidhannagar, Kolkata 700064, India

A. Gibaud
Laboratoire de Physique de l'Etat Condensé, Faculté des Sciences, Université du Maine, 72085 Le Mans, France

C. Sella
Laboratoire d'Optique des Solides, Université de Paris VI, 75252 Paris, France

(Received 23 December 2003; accepted 25 May 2004)

The morphology of $Au-Al_2O_3$ nanocermet thin films, prepared by cosputtering Au and Al_2O_3 on float glass substrates, was studied using surface sensitive x-ray scattering techniques and the results were correlated with the optical absorption of the films measured using ultraviolet visible spectroscopy. The presence of gold nanoparticles in an alumina matrix is evident from both x-ray scattering and spectroscopic studies. The distribution of nanoparticles is obtained from grazing incidence small angle x-ray scattering, while the electron density profile obtained from the analysis of x-ray reflectivity data gives total film thickness, volume fraction (f) of Au and the special arrangement along the growth direction. Optical properties show a linear dependence of the absorption peak position with f, which is interesting for making nanocomposites of tunable absorption. © *2004 American Institute of Physics*. [DOI: 10.1063/1.1774250]

Thin composite films containing metal nanoparticles in a ceramic matrix (known as nanocermets) are of interest for the development of new photonic devices.[1] Nanocermets are particularly important for solar energy conversion in that they tend to exhibit large absorption cross sections near ultraviolet visible (UV–VIS) frequencies.[2] It is well known that when Au is confined it shows strong absorption near the UV–VIS region due to surface plasmon resonance.[3] Au-nanocermet is also a material for the study of nonlinear optical properties.[1] Optical properties of these nanocermet films are however, not only related to the size, but also to the shape and distribution of the nanoparticles in the matrix. Thus by tuning the size, shape, and volume fraction or distribution of nanoparticles in a matrix one can tune the absorption frequency of the material. It is therefore of continuing interest to study the morphology and the optical properties of the films and to correlate these to tailor microstructure to achieve the desired materials properties.

The morphology of nanocermet films is usually determined by electron microscopy, which gives direct but local information. However, a more appropriate approach to describe their morphology would be a statistical one. Furthermore, to correlate the structure or morphology with optical properties it is highly desirable to study the same sample without modification or destruction. Surface sensitive x-ray scattering techniques enable the statistical determination of the morphology of thin films in a nondestructive way.[4] Specular reflectivity provides the structure of a film along the growth direction[5,6] while grazing incidence small angle x-ray scattering (GISAXS) provides the average size, shape, and distribution of nanoparticles in the matrix.[7,8] The combination of reflectivity and GISAXS yields the complete morphological information of the system,[4,9–11] which can then be compared with the optical properties. Here we have used x-ray scattering techniques and UV–VIS spectroscopy to study $Au-Al_2O_3$ nanocermet films.

$Au-Al_2O_3$ cermet films were prepared by sputtering a disk on float glass substrates. The disk was made up of a number of small Au pellets on a big Al_2O_3 disk and the number (n) was varied to get films having different volume fraction (f) of Au. Three such films, labeled as nAu$-Al_2O_3$, where $n=19$, 42, and 84 were prepared. GISAXS measurements of the films were performed using a synchrotron x-ray source (D22 beam line, LURE) at x-ray energy 7 keV and the reciprocal space maps were collected with a two-dimensional (2D) detector for a fixed incidence angle just above the critical angle of film. The same GISAXS measurements were also performed with a 2D GADDS detector in laboratory setup (D8 Discover, Bruker AXS). X-ray specular reflectivity measurements were performed using a laboratory source of x rays with wavelength 1.54 Å. Optical absorption spectra of the films were collected using an UV–VIS spectrophotometer (Cintra 10*e*, GBC).

GISAXS images of the films are shown in Fig. 1. The annular ring observed in the figure is related to the interparticle separation. It is observed from Fig. 1 that as the Au concentration increases the radius of the annular ring decreases, i.e., the interparticle separation (d) increases. The x-ray reflectivity data of the films are shown in Fig. 2. The Kiessig fringes (clearly observed in the inset of Fig. 2) are related to the total film thickness (D),[6] while the peak around $q_z \sim 0.1$ Å^{-1} is related to the interparticle or layer separation (d_L) along the growth direction.

To extract quantative morphological information of the films, the x-ray scattering data have been analyzed considering electron density (ρ) of a thin film in which metal clusters are randomly distributed in an amorphous matrix. For a heterogeneous thin film, where particles (clusters or pores) are randomly distributed in an amorphous matrix, the electron density can be written as[4]

[a)]Electronic mail: shazra@surf.saha.ernet.in

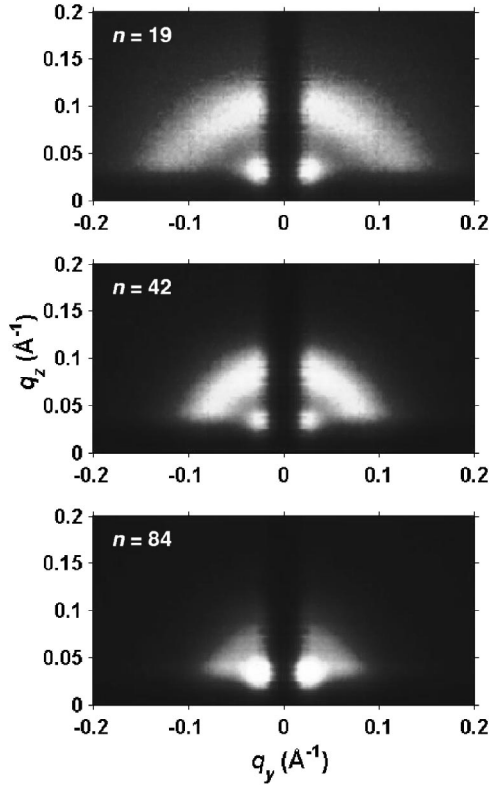

FIG. 1. GISAXS images of $Au-Al_2O_3$ nanocermet films. Radius of the annular ring observed here decreases from top to bottom with the increase of Au concentration.

$$\rho(\boldsymbol{r}) = \left[\rho_m + \Delta\rho \sum_i \delta(\boldsymbol{r} - \boldsymbol{r}_i) \otimes S_p(\boldsymbol{r}_i) \right] S_F(\boldsymbol{r}), \tag{1}$$

where $\Delta\rho = \rho_p - \rho_m$, $\delta(\boldsymbol{r} - \boldsymbol{r}_i)$ is related to the distribution of the particles, $S_p(\boldsymbol{r}_i)$ is related to the shape and size of the ith particle at a position $\boldsymbol{r}_i$, and $S_F(\boldsymbol{r})$ is related to the finite dimension of the film. We assume that part of the incident beam is reflected at the film interfaces and part of it is scattered by particles (which have different electron densities from the matrix). Then in a kinematical approximation the total scattered intensity can be written as the sum of two intensities arising separately from the matrix and the particles (neglecting the matrix-particles cross term) as

$$I(q) = R(q_z) + I_p(q), \tag{2}$$

where $R(q_z)$ is the reflectivity part of the film considering uniform electron density. For actual calculation we have, however, divided each film of thickness D into a number of slices and used a matrix formalism.[5] The reflectivity data thus fitted are shown in Fig. 2 along with the electron density profile. Different parameters obtained are also listed in Table I.

$I_p(q)$ is arising from particles and can be calculated considering size, shape, and distribution of the them in the matrix. If we consider spherical particles of radius R, distributed in the matrix according to a cumulative disorder with average separation d, then[12–14]

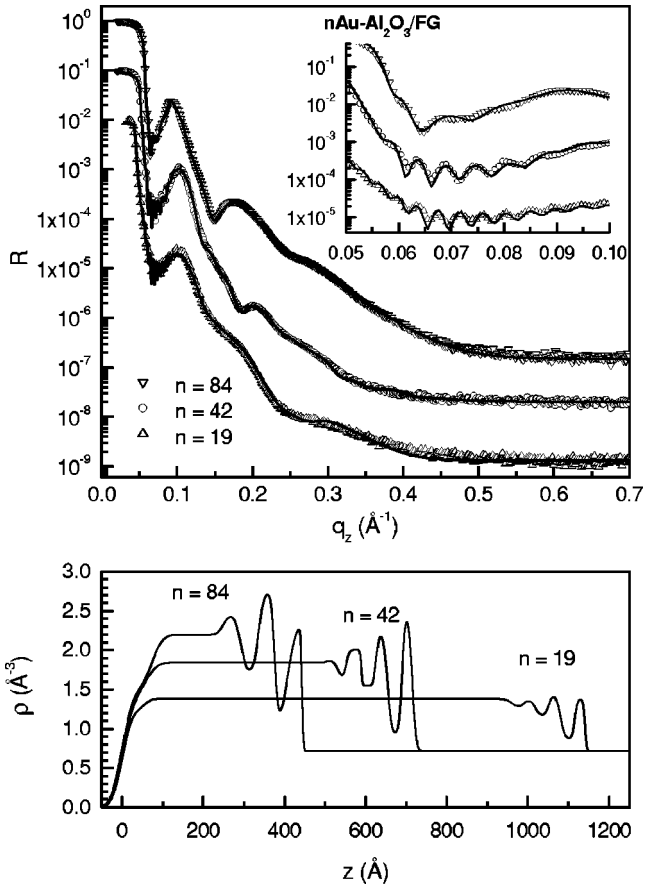

FIG. 2. Top panel: X-ray reflectivity data and fitted curves of $Au-Al_2O_3$ nanocermet films for different Au concentration. Curves are shifted vertically for visibility. Inset shows enlarged selected portion of the curves to show the Kiessig fringes. Bottom panel: Corresponding electron density profiles.

$$I_p \propto \frac{(\sin qR - qR\cos qR)^2}{(qR)^6} \times \frac{1 - e^{-2q^2\sigma_d^2}}{1 - 2\cos(qd)e^{-q^2\sigma_d^2} + e^{-2q^2\sigma_d^2}}, \tag{3}$$

where σ_d is the variance of d. In actual calculation one has to consider the variance of R as well and take into account the effect of reduced dimension of the film. Considering Eq. (3), the particle size and interparticle separation have been calculated other than specular direction, which is listed in Table I.

Optical absorption spectra of three nanocermet films are shown in Fig. 3. The absorption peaks observed in the spectra are due to the presence of Au nanoparticles in the films. Positions of the absorption peak, known as peak wavelength (λ_p), are listed in Table I. λ_p is also plotted in the inset of Fig. 3 as a function of f, which shows linear dependence between them. This suggests that by controlled inclusion of Au in Al_2O_3 matrix one can tune the optical absorption peak position to a desired value within a wavelength window. A strong shift in the peak position has been observed which cannot be explained in terms of simple Mie theory.[15] Shift of the absorption peak with particle size has been observed before.[3] In some cases,[16,17] where the shape of the particles was asymmetrical (say nanorod), two peaks (one for transverse mode and another for longitudinal mode) were present and the shift in the peak for longitudinal mode observed was attributed to the change in aspect ratio of the particles. In

TABLE I. Parameters of $Au-Al_2O_3$ nanocermet thin films obtained from x-ray scattering and optical spectroscopy analysis.

nAu$-Al_2O_3$	Thickness (nm)	f	σ_{top} (nm)	d_L (nm)	$d(\sigma_d)$(nm)	$2R$ (nm)	$d-2R$ (nm)	λ_p (nm)
19	115	0.05	3.9	6.2	5.3 (0.5)	3.4	1.9	523
42	74	0.17	4.0	6.5	6.0 (0.6)	4.7	1.3	566
84	48	0.25	4.1	7.5	~6.8(0.8)	5.9	~0.9	594

other cases,[18] the shape of the particles was nearly symmetrical, and a single peak was present, which shifts with size. However, the size range was much larger compared to our present case (here particle size is less than 6 nm, as listed in Table I) for the peak shift that we observed here. For very small particles, a broadening of the absorption peak with decreasing particle size is usually observed.[1,19] There is no clear explanation for the peak shift with particle size, especially for small metal particles. To explain the shift one has to consider either the change in Drude plasma frequency of the metal particles or the change in the value of the dielectric constant of the matrix. The latter can be explained by replacing the matrix with an effective medium (as done in effective medium theory[3]) where the dielectric constant is expected to increase with the increase of Au concentration. Although a change in the Drude plasma frequency is unlikely, an increase in the Au concentration may increase the particle–particle interaction, which in turn can decrease the effective plasma frequency.

In conclusion, $Au-Al_2O_3$ nanocermet films prepared by cosputtering were observed to show optical absorption in the visible range. The morphology of the films was determined using x-ray scattering techniques, which indicate cumulative disorder (due to the presence of variance, σ_d) in the distribution of Au nanoparticles, especially along the growth direction, starting from the substrate (as suggested by the oscillations in the electron density profile close to the substrate) similar to what is observed with $Pt-Al_2O_3$ nanocermet films.[4] As the volume fraction of Au in the alumina matrix increases, the size of the Au nanoparticles as well as interparticle separation increases. However, the interparticle surface-separation ($d-2R$) decreases, giving rise to strong surface interaction. This, along with the high dielectric constant of the effective medium, shifts the absorption peak position with Au volume fraction.

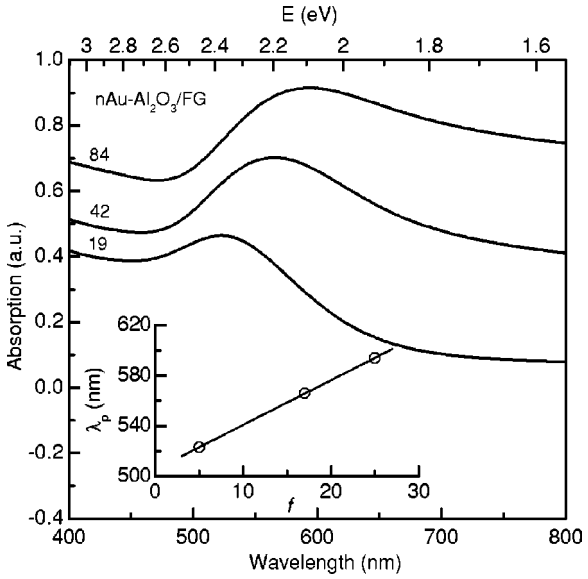

FIG. 3. Optical absorption spectra of $Au-Al_2O_3$ nanocermet films with three different volume fraction (f) of Au. Inset shows variation of absorption peak position (λ_p) as a function of f.

The authors are greatly indebted to the LURE facility and thankful to O. Lyon and A. Naudon for their collaboration during GISAXS measurements.

[1] C. Flytzanis, F. Hache, M. C. Klein, D. Ricard, and P. Roussingnol, Prog. Opt. **XXIX**, 323 (1991).
[2] G. A. Niklasson and C. G. Granqvist, J. Appl. Phys. **55**, 3382 (1984).
[3] S. Link and M. A. El-Sayed, J. Phys. Chem. B **103**, 8410 (1999).
[4] S. Hazra, A. Gibaud A. Desert, C. Sella, and A. Naudon, Physica B **283**, 97 (2000).
[5] A. Gibaud and S. Hazra, Curr. Sci. **78**, 1467 (2000).
[6] M. K. Sanyal, A. Datta, and S. Hazra, Pure Appl. Chem. **74**, 1553 (2002).
[7] A. Naudon and D. Babonneau, Z. Metallkd. **88**, 596 (1997).
[8] C. Revenant, F. Leroy, R. Lazzari, G. Renaud, and C. R. Henry, Phys. Rev. B **69**, 035411 (2004).
[9] T. Roch, V. Holý, A. Daniel, E. Höflinger, M. Meduna, T. H. Metzger, G. Bauer, J. Zhu, K. Brunner, and G. Abstreiter, J. Phys. D **34**, A6 (2001).
[10] A. Gibaud, S. Hazra, C. Sella, P. Laffez, A. Desert, A. Naudon, and G. Van Tendeloo, Phys. Rev. B **63**, 193407 (2001).
[11] A. Gibaud, A. Baptite, D. A. Doshi, C. J. Brinker, L. Yang, and B. Ocko, Europhys. Lett. **63**, 833 (2003).
[12] M. Rauscher, T. Salditt, and H. Spohn, Phys. Rev. B **52**, 16855 (1995).
[13] B. K. Vainshtein, *Diffraction of X-rays by Chain Molecules* (Elsevier, Amsterdam, 1966).
[14] A. Guinier and G. Fournet, *Small-Angle Scattering of X-Ray* (Wiley, New York, 1955).
[15] G. Mie, Ann. Phys. (Leipzig) **25**, 377 (1908).
[16] N. Felidj, J. Aubard, G. Levi, J. R. Krenn, G. Schider, A. Leitner, and F. R. Aussenegg, Phys. Rev. B **66**, 245407 (2002).
[17] S. Link, M. B. Mohamed, and M. A. El-Sayed, J. Phys. Chem. B **103**, 3073 (1999).
[18] S. Link and M. A. El-Sayed, J. Phys. Chem. B **103**, 4212 (1999).
[19] W. P. Halperin, Rev. Mod. Phys. **58**, 533 (1986).